Setting up of a microKelvin refrigerator facility at TIFR

H. R. Naren, R. S. Sannabhadti, Anil Kumar, V. Arolkar, Arlette de Waard, G. Frossati and S. Ramakrishan

In this note, we report the setting up of the first adiabatic nuclear demagnetization facility in India at the Tata Institute of Fundamental Research, Mumbai. It consists of a high cooling power dilution refrigerator to which a 5 kg copper nuclear stage is attached via a superconducting heat switch. We describe details of the design and construction of the various important parts of the refrigerator with relevant background. With the project having been started in 2005–06, we can now reach temperatures as low as 39 mK in this system. Temperature was measured using ruthenium oxide and carbon (SPEER) resistance sensors in the range 4.2 K–20 mK, cerium magnesium nitrate susceptibility sensors in the range 4.2 K–4 mK, and platinum NMR thermometry in the range 20 mK–39 μK. We believe this refrigerator is an important addition to ultra-low temperature physics research in our country.

In the present state of development of low-temperature physics there are, in principle, three methods that are required (and are the most widely used) to span the whole temperature range that has been accessed. Firstly, cooling by evaporation of liquid ^{4}He (^{3}He) down to nearly 1 K (0.3 K). Secondly, cooling by phase separation of ^{3}He–^{4}He mixtures (the dilution refrigerator) down to a few millikelvin. And finally, adiabatic demagnetization of nuclear spins to reach a few microkelvin. In the sub-milliKelvin range one can speak of two different temperatures – the nuclear spin temperature and the lattice temperature. This is because the time taken for the nuclear spin temperature to equilibriate with the lattice and electrons (the spin–lattice relaxation time) could be larger than several hours at such temperatures. The lowest nuclear spin temperatures recorded are as small as 100 pK and the lowest lattice-electron temperatures are as small as 10 μK. Lounasmma and co-workers, building on the pioneering experiments of Kurti *et al*., developed nuclear demagnetization as a feasible technique in the 1970s (see ref. 1 and references therein). Nuclear cooling required the development of powerful dilution refrigerators and superconducting magnets to become a practical method of cooling. We describe here our efforts towards the setting up of an adiabatic nuclear demagnetization refrigerator at the Tata Institute of Fundamental Research (TIFR), Mumbai, a first such effort in India, thus opening up the microkelvin range for condensed matter physics experiments.

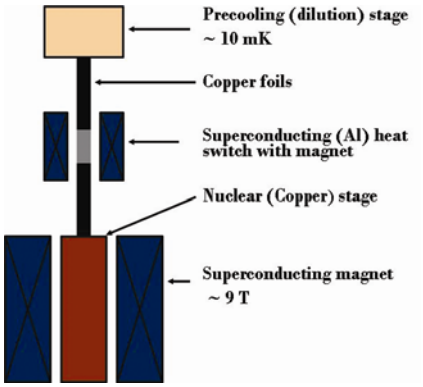

Figure 1. Schematic of an adiabatic nuclear demagnetization set-up.

A schematic of nuclear refrigeration is shown in Figure 1. It consists of a precooling stage which in our case is a high cooling power dilution refrigerator. This is connected to the copper nuclear stage via a superconducting heat switch. The dilution refrigerator was bought from Leiden Cryogenics. The superconducting heat switch, copper nuclear stage and the platinum NMR thermometer were designed by us and fabricated by Leiden Cryogenics (http://www.leidencryogenics.com/).

Steps of cooling

The basic operation consists of several steps of cooling as indicated below.

Step 1: The system is pre-cooled in liquid nitrogen for a day. Then liquid nitrogen is removed and the system is immersed in a liquid helium bath for another day to effectively cool the cryostat and the magnet. It takes nearly 100 l of liquid helium to precool to 4.2 K and less than a litre an hour afterwards.

Step 2: Pumping over liquid helium takes it down to 1.4 K. This is done by means of a 1 K pot into which liquid helium is allowed through capillaries (controllable by a needle valve) and pumped by means of a dedicated pump. This takes the system to 1.4 K from 4.2 K in ~15 min.

Step 3: ^{3}He and ^{4}He are taken out of their dumps and successively condensed in the refrigerator. This takes nearly 6 h.

Step 4: Pumping over (predominantly) liquid ^{3}He (which results automatically during condensation) takes the mixture below the phase separation temperature of the ^{3}He–^{4}He mixture (0.8 K).

Step 5: By ensuring that the phase separation occurs in the mixing chamber using a heater on the still (described in the next section), the mixture is circulated by means of powerful pumps and gradually the mixing chamber reaches a base temperature of 8 mK in a day.

Step 6: Adiabatic demagnetization is performed on the copper stage by means of a 9 T magnet to reach temperatures of a few tens of microkelvin.

The dilution refrigerator

The dilution refrigerator we used is a commercial one (DRS 1000) bought from Leiden Cryogenics. Figure 2 shows the three main parts of this system – the dilution insert, the ^{3}He dump, valve system and pumps, and the ^{4}He dump. The system has a large cooling power: Q_{120mK} ~ 1300 μW and Q_{30mK} ~ 80 μW. Without the copper nuclear stage it reaches a base temperature of ~4.5 mK. A Pfeiffer DUO-20 rotary pump is used for the 1 K pot. Two Varian 551 turbo pumps (cooled by chilled water) are used for mixture circulation and they are backed by an Edwards XDS35 (oil-free) scroll pump. The main valves are controlled pneumatically and the rest are solenoid valves. The pumps and the

microprocessor-based valve control system are housed together in a compact arrangement whose frame acts as the ^{3}He dump (of capacity ~176 l). There is a separate ^{4}He dump of capacity ~600 l. Figure 3 shows an expanded view of the dilution refrigerator stages where as one progresses downwards from the 4 K plate, which is in direct contact with the liquid helium bath, the temperature goes down gradually. The wires from the top are anchored at every stage to ensure good heat sinking. The system also has a charcoal cryopump arrangement on the 1 K plate (not shown in the figure), which consists of porous charcoal with a heater to facilitate initial desorption. The space in the insert (IVC) is initially checked for leaks with a leak detector, then pumped with a turbo pump and the final stages of pumping are taken over by the charcoal cryopump. The operating vacuum is around 10^{-6} mbar.

The 1 K stage and the still are provided with ruthenium oxide temperature sensors and the mixing chamber is provided with a SPEER resistance sensor and a cerium magnesium nitrate (CMN) susceptibility sensor. The resistance sensors are measured using an AVS-47 bridge and the CMN is measured using a mutual inductance bridge. The still is also provided with a heater to maintain it slightly above the phase separation temperature. The level of mixture in the still is monitored using a capacitance gauge. The rate of circulation is measured using a flowmeter (McMillan Company). The whole condensation and circulation process can be performed either by manual operation of valves and pumps, or by an automatic microprocessor-based programme. The system has to be optimized in terms of still mixture level and circulation rate to reach the base temperature. We could reach a base temperature of around 4 mK without any load on the mixing chamber and around 8 mK with the copper nuclear stage attached.

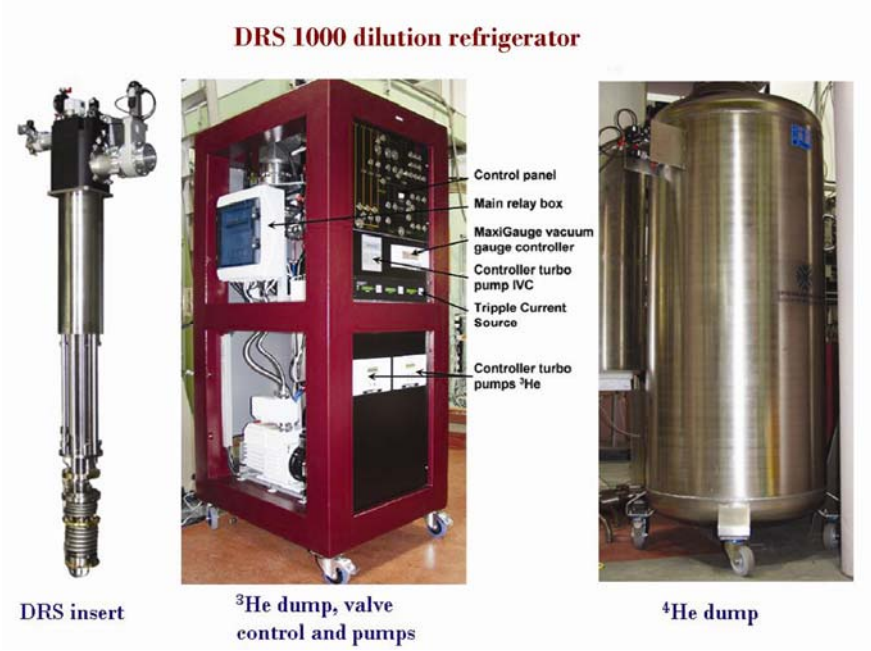

Figure 2. The DRS1000 dilution refrigerator. (Left) Dilution insert. (Middle) Pump housing, valve system and ^{3}He dump. (Right) ^{4}He dump.

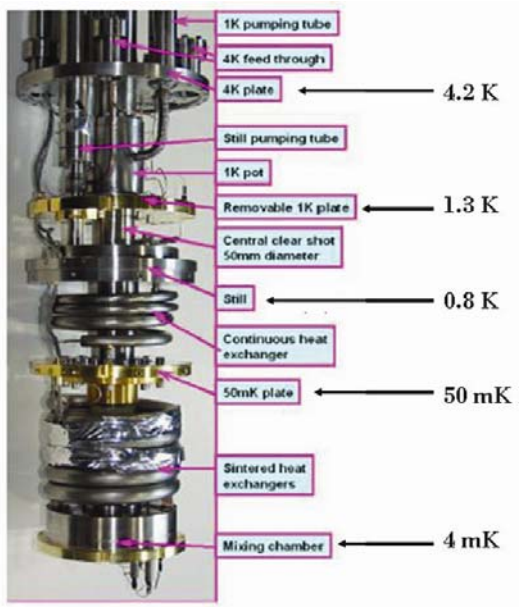

Figure 3. The dilution refrigerator stages showing a gradual lowering of temperature from the top 4 K plate.

Principles of nuclear cooling

The basic steps in nuclear cooling are isothermal magnetization and adiabatic demagnetization. Figure 4 shows the entropy versus temperature curves of the nuclear spin system of copper at different fields[2]. The arrows indicate the processes involved. With the superconducting heat switch closed, the copper stage is magnetized in the 9 T magnet. This change in entropy heats up the stage. Since the switch is closed, the high power dilution stage cools back the copper stage to ~10 mK in typically a day. This is the isothermal magnetization part. After this, the heat switch is opened and the copper stage is demagnetized adiabatically to a final field of a few millitesla over 2 to 3 days. Demagnetization has to be slow enough to let the system equilibriate at every point. This is done by ensuring that B (magnetic field) versus T (temperature) is linear by setting the ramp-down rate of the magnet appropriately. In an ideal adiabatic demagnetization,

$$T_{\mathrm{f}} = \frac{T_{\mathrm{i}}}{B_{\mathrm{i}}}\sqrt{B_{\mathrm{f}}^2 + b^2},$$

where f refers to final and i to initial. b is the internal field of the nuclear spins.

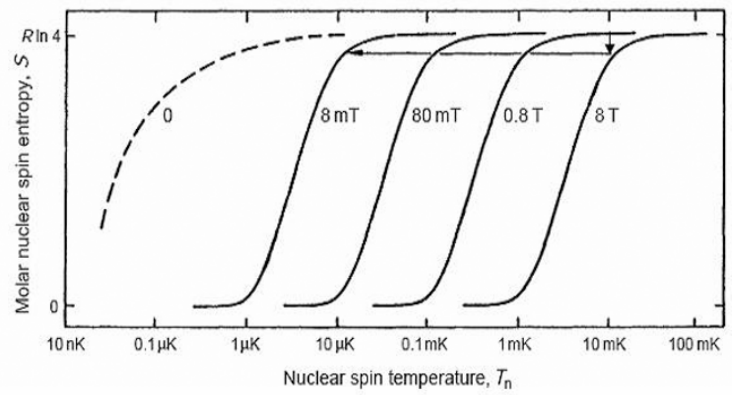

Figure 4. Entropy versus temperature curves of the Copper nuclear spin system at different fields[2].

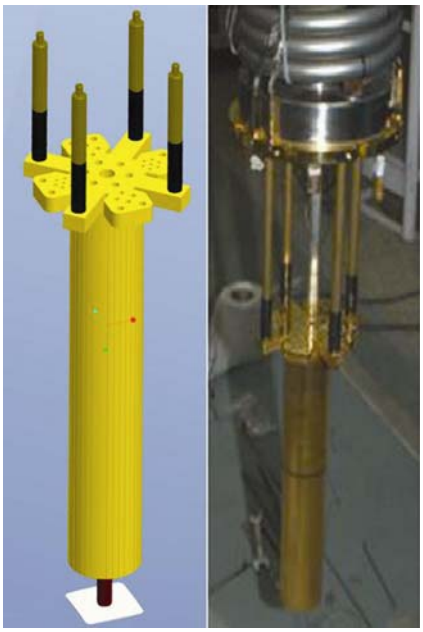

Figure 5. (Left) Diagrammatic sketch of the copper nuclear stage. (Right) Actual copper stage in our laboratory.

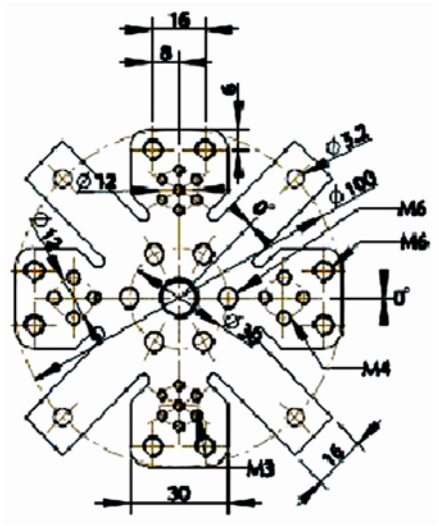

Figure 6. Threaded holes on the copper stage for mounting experiments.

Thus a large B_i/T_i is necessary for a small T_f. The smallness of the nuclear moments implies that the Zeeman splitting between the energy levels even in an initial field of 8 T is around 4.4 mK (for copper). Thus at initial temperatures of 10 mK, the change in entropy between the magnetized and unmagnetized state is only about 9%. For copper (spin 3/2), with $T_i \sim 6$ mK, $B_i \sim 8$ T and $B_f \sim 8$ mT, the final temperature reached is ~6 μK (ideally). In the above final state, the Zeeman splitting between the energy levels is ~4.4 μK. Thus setting lower B_f values will reduce the cooling power of the fridge, since the cooling power is derived from the extent of Zeeman splitting.

Design of nuclear stage

The choice of material for the nuclear stage involves various considerations[2].

- It should be a good metal since we require a small spin–lattice relaxation time and good thermal conductivity (κ).
- It should not be superconducting in the temperature range of interest.
- It should be available in high purity.
- Its electronic spins should not order in the temperature range of interest.
- It should have most of its isotopes with nuclear spin > 0.
- Its nuclear ordering temperature (T_{nc}) and internal field (b) must be as low as possible.

Hence the most popular choice is copper. It satisfies all the above requirements. It has a $T_{nc} < 0.1$ μK, $b \sim 0.36$ mT and both isotopes have spin 3/2.

Our copper stage (shown in Figure 5) is around 5 kg in mass (80 moles), 50 mm in diameter and 300 mm in length. It is made of 99.99% electrolytic copper (of the type NOSV, from Aurubis, Germany) with a residual resistivity ratio ≥ 400. It is gold-plated and has 36 slits running for 290 mm along the length to reduce eddy current heating. The magnetic field profile is such that around 75% of the stage experiences larger than 75% of the maximum field. The magnetic field is compensated such that beyond the coil region, the residual field is lesser than a few gauss. The top surface of the copper stage has a number of threadable holes (Figure 6) to mount experiments. It is connected to the mixing chamber via four legs (and the heat

switch) with joints made of 'Vespel', which is a commercial polymer-based material with very low thermal conductivity.

Design of superconducting heat switch

In the superconducting state, materials have bad thermal conductivity. That is because of the reduction in the number of electrons available for thermal conduction; electrons form Cooper pairs in a superconductor. This fact is utilized to form a heat switch out of a superconductor. We can see the difference (Figure 7) in thermal conductivity in the normal and superconducting state for aluminium. In fact, the thermal conductivity of aluminium becomes comparable to 'epibond' – a polymer – at very low temperatures. At $T < 0.1T_c$, the thermal conductivity is mainly phonon-mediated and the ratio of the normal to superconducting state thermal conductivity – the switching ratio (κ_n/κ_s) is

$$\kappa_n/\kappa_s \sim 0.05\,(\theta_D/T)^2,$$

where θ_D is the Debye temperature of the material. Therefore, the requirements of a good heat switch material are a large switching ratio, availability in high purity, large θ_D and a reasonably low critical field so that it does not require a large current to be passed in the coil to drive it normal. Hence aluminium happens to be a good choice. It has a T_c = 1.1 K, critical field H_c = 10.5 mT and θ_D = 400 K.

Our heat switch (schematic shown in Figure 8) was made by diffusion-welding 0.2 mm thick and 13 mm wide copper foils (the same type of copper as the nuclear stage) to 0.2 mm thick pure aluminium foils (type 'Specpure' of Johnson Matthey with 6 N purity). The Cu and Al foils were pressed using a stainless-steel jig with molybdenum bolts and heated under vacuum for 12 h at 400°C. The free length of the Al foils was about 10 mm, with two lengths of 10 mm overlapping the copper foils. Multiple foils (30 in our case) are required to reduce eddy current heating as well as κ_s (since mean free path of phonons ~ sample dimensions at such temperatures). The Al foils are parallel to the field. The superconducting switch field coil was made of 75 μm Nb–Ti in Cu matrix wire with 7269 turns on a brass mandrel, giving a field of 2970 gauss/ampere (requires ~0.15 Amp to turn aluminium normal). The coil was shielded from fringe fields with a Nb cylinder 50 mm long. While ramping the field down to zero, we oscillate it with a reducing amplitude to eliminate the trapped flux. We have obtained switching ratios > 60,000.

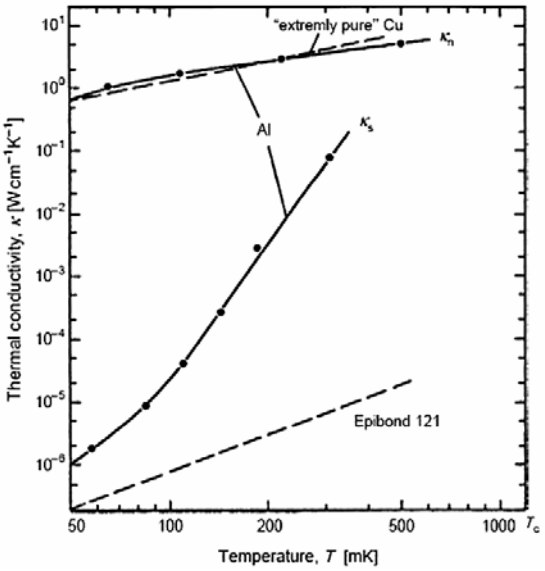

Figure 7. Thermal conductivity of superconducting and normal aluminium along with that of copper and 'epibond'[2].

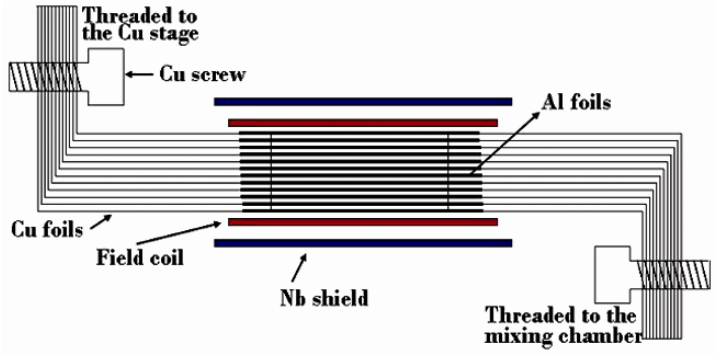

Figure 8. Schematic of the superconducting heat switch.

Thermometry

The dilution fridge temperatures are measured using a CMN mutual inductance thermometer, where the mutual inductance ($M(T)$) of the coil containing CMN varies according to Curie–Weiss law:

$$T = \frac{C}{M(T) - M_0}.$$

The CMN is initially calibrated with respect to the SPEER resistance thermometer as shown in Figure 9. Whereas the

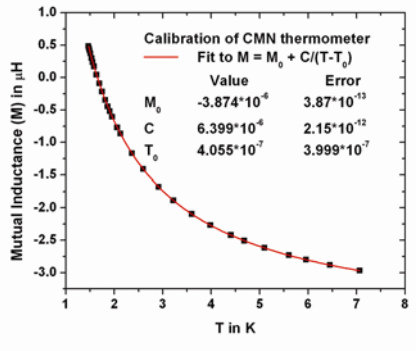

Figure 9. Initial calibration of the cerium magnesium nitrate (CMN) susceptibility thermometer against the SPEER resistance thermometer according to Curie–Weiss law. T_0 is very small and is therefore neglected.

Curie constant (C) does not change significantly with every run, M_0 needs to be determined in every run and this is done by a calibration at 4.2 K.

Below 10 mK thermometry is performed using a platinum (^{195}Pt, the only nuclear magnetic isotope of Pt (spin = 1/2)) NMR thermometer. Our Pt thermometer (Figure 10) was made of 4000 pure Pt wires 20 μm in diameter and around 8 mm in length, with the NMR excitation coil being made of 770 windings of 25 μm copper wire with inductance ~1.3 mH. The Pt wires were wound (2000 turns) on a Teflon mandrel, then cut and folded to give a bundle of 4000 wires. The bundle of 2.7 mm diameter was pulled through a silver cylinder extending about 10 mm further from the cylinder. The silver cylinder was then swaged using a lathe three-claw mandrel and was then machined leaving a 3 mm long conical piece. This cone was then pressed into a steel cylinder with a 2.7 mm hole with a slightly conical end and welded to form a spherical cap. Welding was done as fast as possible using a current of 20 A on a tungsten inert gas welder. The bundle was then removed from the steel cylinder and hammered into a horizontal hole made on a 4 N purity silver rod-holder with an M5 threaded end which gets threaded on the Cu stage. The thermometer was then annealed at 800°C for 12 h in air. The NMR coil was then fixed with a small amount of super-glue (Cyanoacrylate) to the silver post. The field coil was made of 67 μm Nb–Ti in Cu matrix wire with 8610 turns giving 3620 gauss/ampere wound on a brass mandrel. A niobium cylinder was fixed on it for shielding from fringe fields.

Figure 10. Platinum NMR thermometer mounted on a silver holder.

In NMR measurements, there are two important timescales: t_1, the nuclear spin–lattice relaxation time and t_2, the nuclear spin–spin relaxation time ($t_2 \sim 1$ ms for Pt). The platinum spins are magnetized in the static magnetic field (taken along the z-direction). These spins are tipped in a perpendicular direction through an excitation pulse (Figure 11). With a large enough pulse the spins can be completely tipped and the magnetization along the tipping direction in the xy plane is maximum. But within a short time (t_2), the spins decohere in the xy-plane and the magnetization M_{xy} decays rapidly as:

$$M_{xy}(t) = M_{xy}(0) * \exp(-t/t_2).$$

This gives what is known as a free induction decay (FID) curve, as shown in Figure 12. The FID curve is preceded by several tipping pulses as visible in the figure. The magnetization however continues to increase along the z-direction after tipping and this goes as:

$$M_z(t) = M_{z,\mathrm{eq}}(1 - \exp(-t/t_1)).$$

The spin–lattice relaxation time t_1 is inversely proportional to the temperature as

$$T * t_1 = K,$$

where K is known as the Korringa constant (~30 mK∗sec for Pt). Once K is obtained by calibration, thermometry can be performed in what is known as the Korringa mode by measuring t_1. However, the Korringa mode causes heating due to the tipping pulses and hence it is done once at high temperatures (~10 mK) to obtain the Curie constant (C) of the Pt spins. At lower temperatures the measurement mode is known as Curie mode, where the magnetization (M_z) is measured to directly give the temperature from

$$T = C/M_z.$$

The ordering temperature T_0 for Pt is <1 μK and hence is neglected in the above relation. In Figure 13, we show the various cooling mechanisms in play. While adiabatic demagnetization cools the nuclear spins, this is conducted to the electrons via the hyperfine interaction. Then the lattice cools down via the

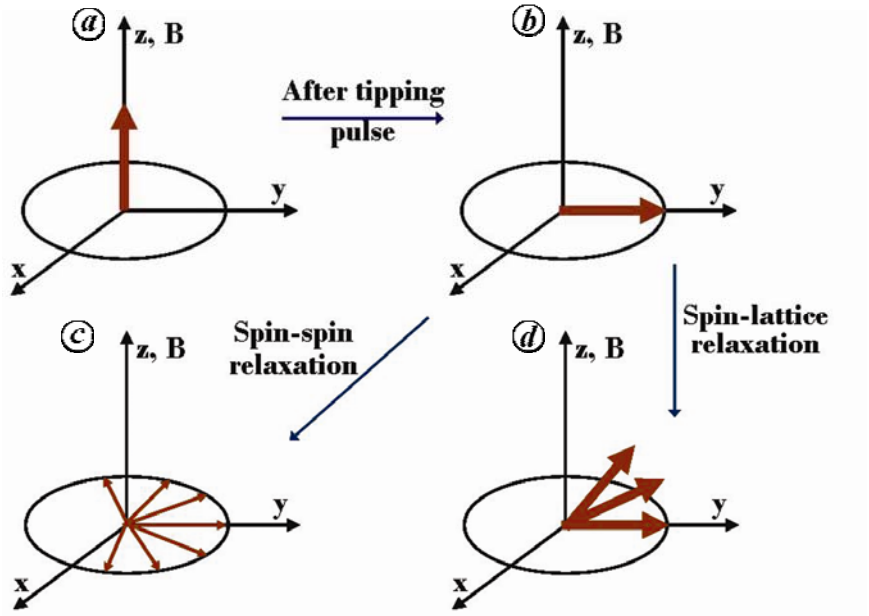

Figure 11. Processes in NMR measurements. ***a***, Spins all aligned with the static field along z-axis producing $M_{z,\mathrm{eq}}$. ***b***, Spins tipped to the x-axis due to application of a tipping pulse producing $M_{xy}(0)$. ***c***, Spins decohering in the xy-plane causing M_{xy} to average to zero after several spin–spin relaxation timescales. This gives the free induction decay curve. ***d***, Spins (made coherent at every point by small pulses) relaxing to $M_{z,\mathrm{eq}}$. This takes several spin–lattice relaxation times.

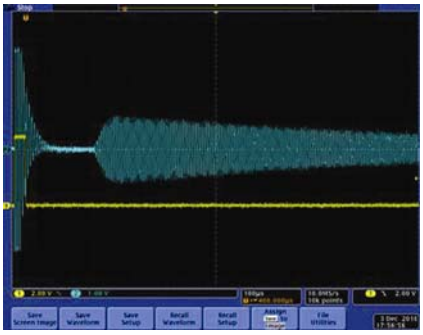

Figure 12. Free induction decay (FID) curve at 39 μK. Notice the excitation pulses before the FID curve.

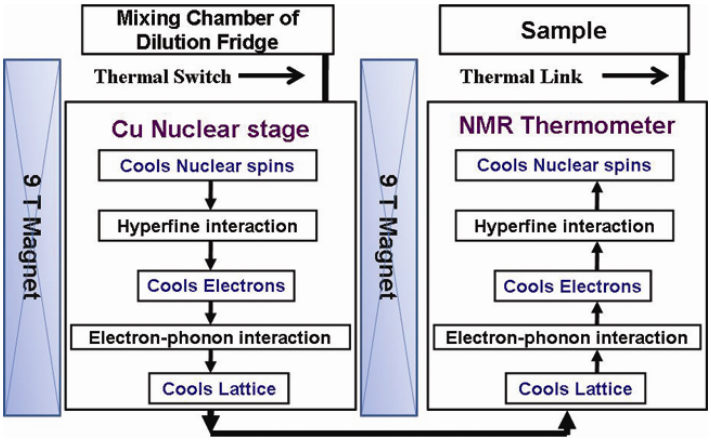

Figure 13. Various cooling mechanisms at play in nuclear cooling and NMR thermometry.

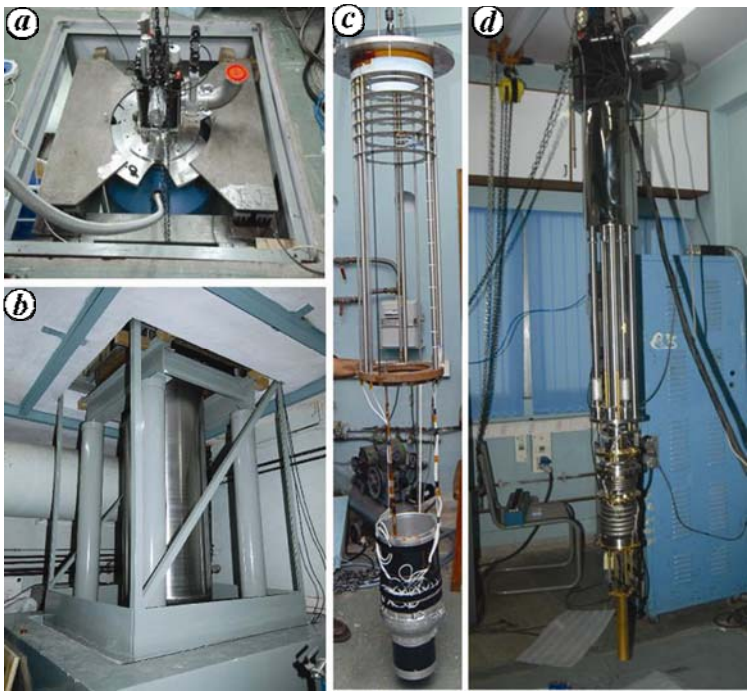

Figure 14. ***a***, Cryostat mounted on active vibration isolation pads. ***b***, Cryostat hanging into the basement on pillars resting on a sand-bed. ***c***, Magnet insert. ***d***, Dilution insert with the copper stage.

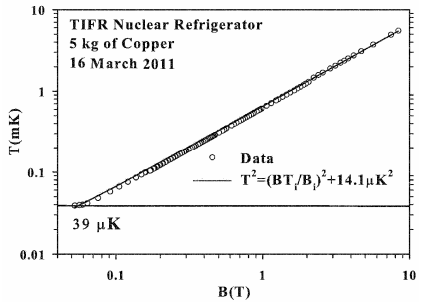

Figure 15. The *B* versus *T* curve during demagnetization. The continuous line is a fit to eq. (1) in the text.

electron–phonon coupling. The reverse happens when the temperature is measured by NMR thermometry. It is crucial to keep the sample thermally linked to the thermometer for accurate measurements.

Instrument housing and vibration isolation

The refrigerator insert (Figure 14 *d*) sits in an outer magnet insert (Figure 14 *c*) which in turn sits in a fibre-glass cryostat. The cryostat hangs into the basement (Figure 14 *b*) on two active vibration isolation pads (Figure 14 *a*) which are mounted on pillars resting on a sand-bed in the basement (Figure 14 *b*). The cryostat is electromagnetically shielded with mild-steel sheets in the basement. Mechanical vibrations are a source of heating and need to be minimized. Our cryostat is essentially mounted in the basement where the building noise is minimum. The sand-bed cuts out further vibrations. The active vibration isolators (Halcyonics, Duo 73) efficiently cut off frequencies below 200 Hz. The damping levels are 95% below 5 Hz and 98% above it. Load capacity of the isolators is 800 kg. The pump vibrations are reduced by wall-mounting the large circulation line.

Successful cooldowns

The refrigerator reached temperatures of 39 μK in March 2011. The temperature was measured with the platinum NMR thermometer (NMR frequency of 193.36 kHz).

We could maintain the system at that temperature for longer than 48 h. The *B*/*T* curve plotted in Figure 15 is fairly

linear, except below 0.1 mK. The reason for this is that the t_1 of copper is larger than 3 h at such temperatures and our power supply ramp rate cannot be reduced below 1 mA/s, and this limits adiabaticity. The heat leak in this system was measured to be <1 nanoWatt (nW) and the expected cooling power is ~ few nW.

Planned experiments

We are at a stage where experiments can be performed at ultra low temperatures. Some of the planned experiments are as follows.

- Reentrant superconductivity in mesoscopic samples of Nb–Ag and Nb–Au planar junctions[3].
- Study of ground state of metals and alloys (e.g. lithium and magnesium for superconductivity)[4,5].
- Granular superconductivity in materials like platinum[6].
- Coexistence of nuclear magnetism and superconductivity as in $AuIn_2$ (ref. 7).
- Two-dimensional metal–insulator transition in semiconductor structures[8].

1. Gloos, K., Smeibidl, P., Kennedy, C., Singsaas, A., Sekowski, P., Mueller, R. M. and Pobell, F., *J. Low Temp. Phys.*, 1988, **73**, 101–136.
2. Pobell, F., *Matter and Methods at Low Temperatures*, Springer, 2007, 3rd edn.
3. Visani, P., Mota, A. C. and Pollini, A., *Phys. Rev. Lett.*, 1990, **65**, 1514–1516.
4. Tuoriniemil, J. *et al.*, *Nature*, 2007, **447**, 187–189.
5. Bucher, E. *et al.*, *Phys. Rev. B*, 1972, **6**, 103–110.
6. König, R., Schindler, A. and Herrmannsdorfer, T., *Phys. Rev. Lett.*, 1999, **82**, 4528–4531.
7. Herrmannsdörfer, T., Smeibidl, P., Schröder-Smeibidl, B. and Pobell, F., *Phys. Rev. Lett*., 1995, **74**, 1665–1668.
8. Kravchenko, S. V. and Sarachik, M. P., *Rep. Prog. Phys*., 2004, **67**, 1–44.

ACKNOWLEDGEMENT. We thank Bhanu Prakash Joshi and all the support staff at TIFR, Mumbai for their help and cooperation during different stages of this project.

Received 11 April 2011; accepted 4 May 2011

H. R. Naren, R. S. Sannabhadti, Anil Kumar, V. Arolkar and S. Ramakrishan are in the Tata Institute of Fundamental Research, Mumbai 400 005, India; Arlette de Waard and G. Frossati are in the Kamerlingh Onnes Laboratory, Leiden University, 2300 RA Leiden, The Netherlands. *e-mail: nareni@tifr.res.in*